



# Parametric study of horizontally vibrated grain packings - Comparison between Discrete Element Method and experimental results

Sébastien Nadler, Olivier Bonnefoy, Jean-Marc Chaix, Jean-Louis Gelet

## ► To cite this version:

Sébastien Nadler, Olivier Bonnefoy, Jean-Marc Chaix, Jean-Louis Gelet. Parametric study of horizontally vibrated grain packings - Comparison between Discrete Element Method and experimental results. *European Physical Journal E: Soft matter and biological physics*, EDP Sciences: EPJ, 2011, 34 (6), pp.66. <10.1140/cpje.i2011-11066-y>. <hal-00608038>

**HAL Id: hal-00608038**

**<https://hal.archives-ouvertes.fr/hal-00608038>**

Submitted on 12 Jul 2011

**HAL** is a multi-disciplinary open access archive for the deposit and dissemination of scientific research documents, whether they are published or not. The documents may come from teaching and research institutions in France or abroad, or from public or private research centers.

L'archive ouverte pluridisciplinaire **HAL**, est destinée au dépôt et à la diffusion de documents scientifiques de niveau recherche, publiés ou non, émanant des établissements d'enseignement et de recherche français ou étrangers, des laboratoires publics ou privés.

# Parametric study of horizontally vibrated grain packings

## Comparison between Discrete Element Method and experimental results

S. NADLER<sup>1</sup>, O. BONNEFOY<sup>1</sup>, J.-M. CHAIX<sup>2</sup>, G. THOMAS<sup>1</sup>, and J.-L. GELET<sup>3</sup>

<sup>1</sup> Ecole Nationale Supérieure des Mines de Saint Etienne, Centre SPIN, LPMG FRE 3312, 158 Cours Fauriel - 42023 Saint-Etienne Cedex 2, France

<sup>2</sup> Laboratoire SIMAP, UMR 5266, Grenoble INP-CNRS-UJF, rue de la piscine, BP 75 - F-38402 St Martin d'Hères cedex, France

<sup>3</sup> Mersen, 6 rue Vaucanson, 69720 St Bonnet de Mure, France

Received: date / Revised version: date

**Abstract.** Numerical and experimental studies have been undertaken to analyze three parameters controlling the compaction of granular media submitted to sinusoidal horizontal vibrations. We have characterized the influence of the dimensionless acceleration  $\Gamma$ , the geometry of the container and the friction coefficients on the grain velocities and on the packing densities. Above a critical acceleration  $\Gamma_{crit}$ , the velocities increase with  $\Gamma$ . For low values of  $\Gamma$ , the surface layers are compacted, whereas the bottom layers remain at their initial density. For high values of  $\Gamma$ , the bottom layers get compacted, the surface layers are fluidized so that the bulk dynamic and relaxed densities decreased. In the same way, the effect of the dimensions of the container and of the friction coefficients on the packing properties has been studied for given heights of sand, acceleration and frequency. It has been shown that the influence of the two last parameters is similar to that of acceleration. The numerical results given by the Discrete Element Method appear to be in good agreement with experimental results.

**PACS.** granular medium – compaction – horizontal vibrations – friction – acceleration – Discrete Element Method – density – velocity – experiment – simulation

## 1 Introduction

### 1.1 Industrial context

Vibrations-based processes are frequently used in industry to compact granular packings. For instance, in building and civil engineering works, vibrating rolls or vibratory plate compactors are used to compact and stabilize soils. Vibrations are also used in food industry; by lowering the apparent volume of granular packings, the packaging and transport costs are reduced. In electrical protection, a field that has inspired this study, vibrations or taps are used to densify and homogeneously arrange sand grains around a silver blade so that the electrical arc is extinguished properly in case of overload.

The industrial know-how, often empirically obtained in a narrow operating window, usually suffers from poor scientific understanding and thus cannot be optimized or surely extrapolated to new designs. It is hence far from easy to choose the vibrations parameters that optimize the densification process in a given situation (grains population, container geometry and dimensions ...).

### 1.2 Literature survey

From a scientific point of view, numerous works have explored granular systems submitted to periodic mechanical solicitations, either with experiments or computer simulations.

Their phenomenology appears highly governed by the intensity of the mechanical excitation, which can be quantified by  $\Gamma$ , the maximum acceleration adimensionnalized by the earth gravity  $g$ . Vertical and horizontal vibrations exhibit the same sensitivity to  $\Gamma$  :

For gently driven systems, *i.e.*  $\Gamma$  below or close to 1, a densification process is usually observed. During a seminal experiment lead by the Chicago laboratory on spherical beads submitted to vertical taps, a logarithmic decrease of the global packing density has been reported (Nowak *et al.* [1], Knight *et al.* [2]). In the commonly accepted explanation, the mechanical energy input induces a local and temporary stress release that allows the granular column to unjam. In this state, grains can roll, slide or move freely, thus exploring a new configuration that will be selected if the gravitational potential energy of the associated packing is lowered. The kinetic behaviour of such a process has been compared to glass relaxation [1]. This

---

Send offprint requests to: O. BONNEFOY

Correspondence to: bonnefoy@emse.fr

experiment has been further analyzed in details by many authors. For instance, Philippe *et al.* [3,4] have shown by Monte-Carlo simulations that a negative vertical gradient of the packing fraction was induced by vibrations.

For vigorously driven systems, *i.e.*  $\Gamma$  above 1 and below a fuzzy threshold around 3, densification is not anymore the predominant phenomenon. In some or all regions of the granular packing, because of the high energy input level, the system is not moving continuously in the configuration space towards a denser state but is “re-initialized” at each period, loosing memory of any previous minimization of its potential energy. In this state, convection can arise.

For higher accelerations, *i.e.*  $\Gamma$  above 3, convection becomes the predominant effect, the grain packing is fluidized and the global density decreases [5–7].

Numerous driving mechanisms have been identified to explain the convection: a sufficiently high negative vertical gradient of the packing as described above [1,2], hysteretic phenomena like those induced by sawtooth shaped vibrating walls [8], collision inelasticity evidenced for instance in ratchet convection [9]. In the present study, convection appears because of another mechanism, namely avalanching. This driving mechanism has been reported by Tennakoon *et al.* [10] in the case of horizontal vibrations and precisely detailed by Raihane *et al.* [5–7].

The convective patterns of vibrating granular media are amazingly various. Here, for sake of conciseness, we only report literature results concerning horizontally vibrated systems. In a numerical study on a 2D granular medium combining a hard sphere model and particle dynamics, Liffman *et al.* [11] showed that, under horizontal vibrations, there is one single convection roll for  $\Gamma < 1$  and two counter-rotating convection rolls for  $\Gamma > 1.2$ . In this second case, grains are moving upwards along the lateral walls. The experimental work conducted by M. Medved *et al.* [12] showed two counter-rotating convection rolls in the upper part of a horizontally vibrated bed, and even four counter-rotating convection rolls for particular situations (highly frictional walls and large values of  $\Gamma$ ). They also noticed that the number of convection rolls depends on the filling height to container length ratio. In our laboratory, vertical and horizontal vibrations have been experimentally investigated by Rouèche *et al.* [13] and Raihane *et al.* [5–7,14] respectively. Whatever the vibrations direction, it has been observed that two counter-rotating rolls appear, in the opposite way of [11]: grains are moving downwards along the lateral walls and upwards in the central region. Concerning the competition between densification and convection processes, experiments carried out on an initially loose sand grains packing vibrated in a rectangular container, [5–7] have shown that the global packing density is maximized for a given value of the acceleration. The authors hypothesized the existence of a maximum as follows. With increasing acceleration, a densification front moves downwards and the thickness of the granular packing able to be densified increases. In parallel, convection gradually develops in the upper part and pre-

vents the densification process in this area. These conclusions are close to those established by Richard *et al.* [15] in the case of a vertically vibrated granular media. The main difference between vertical and horizontal vibration appears to be the lift up of the granular medium: in vertical solicitations, the whole sand packing unjam easily at low acceleration ( $\Gamma = 3$  for  $f=50$  Hz,  $\Gamma = 2$  for  $f=20$  Hz [13]).

After this phenomenological literature survey, let us focus on the numerical method used in this study. The Discrete Element Method (DEM) elaborated by Cundal *et al.* [16] is now a classical tool in granular media problems and gives good agreements with experiments even for complex processes. For instance, Delaney *et al.* [17] studied industrial processes combining a granular flow, segregation and vibration effects and Cleary [18] reported large scale DEM simulations. To our knowledge, few laboratories are using this method to study dense vibrated granular media. We report that Yao *et al.* [19] have used DEM in order to model the influence of high frequency vertical vibrations (600-1200 Hz) on the densification of granular media. Matchet *et al.* [20] have compared DEM and experimental results concerning the energy loss by vertically vibrated granular media, and have shown that this method is partially satisfying since the calculation of the applied force was not successful.

Close to DEM, another method called “Molecular Dynamics”, is also used for studying various phenomena. In this method, Coulomb friction is differently implemented and the rotation of particles is neglected [21]. Gallas *et al.* have employed this method to study the influence of vertical vibrations on a granular medium. It has been reported that the friction, the geometry, the presence of an obstacle [22] and the dissipation coefficient [21] have a large influence on the behaviour of the medium. The segregation phenomenon can also be reproduced by this method [23]: for a big sphere immersed in a medium, no segregation occurs for the lower frequencies ( $f \leq 20$  Hz), segregation has been evidenced for  $f \approx 40$  Hz, and a more complex behaviour for  $f \geq 50$  Hz (up and down displacements of the big sphere). Saluena *et al.* have shown that the dissipation coefficient also has a major influence on the shape and intensity of the convection rolls in horizontally vibrated granular media [24]: the intensity of the convection rolls, their number and direction can change when varying these parameters. We must notice that numerical results are not systematically compared with experimental results.

As a consequence, we think that the study of a vibrated dense granular medium combining experimental and DEM modeling, is an interesting contribution to the literature.

### 1.3 Issues

In the previous section, we have mentioned that  $\Gamma$  presents a great influence on the vibrated granular system. This influence will be studied in this paper both experimentally and by simulation. Other parameters as the frequency  $f$ , the amplitude of the vibration  $A$ , the recipient geometry,

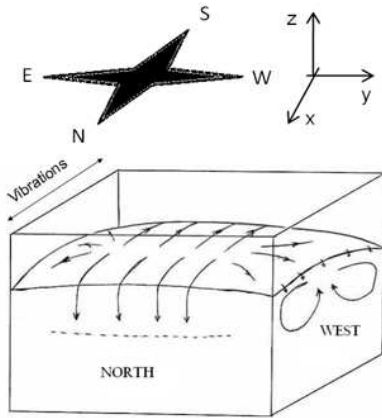


**Fig. 1.** Counter-rotating convection rolls observed experimentally when  $f=50$  Hz and  $\Gamma > 1.5$

the vibrations direction, the grains size and mass, (...), are somewhat less studied. Hereafter we have chosen to characterize the influence of two other parameters: the container length (in the direction of the vibrations) and the friction coefficients  $\mu_{grain/grain}$  and  $\mu_{wall/grain}$ .

The influence of these three parameters is presented in this same paper in order to show the similarities of the response when varying one of them. The studies concerning the influence of  $\Gamma$  and of the container size combine laboratory experiments and numerical simulations. The influence of the friction coefficients is mainly studied with DEM.

## 2 Materials and methods

### 2.1 Experimental set-up and materials

Our experimental conditions are inspired by the industrial manufacturing process of electrical fuses, which are made out of a ceramic recipient containing a silver blade with sand grains in-between. Here, we use a rectangular recipient driven horizontally by an electromagnetic vibrator. The delivered force is continuously adjusted so that the motion is sinusoidal, with a frequency  $f=50$  Hz. The forcing intensity is described by the peak acceleration. More conveniently, we use the dimensionless acceleration  $\Gamma = A(2\pi f)^2/g$ , where  $A$  is the amplitude of oscillations and  $g$  the earth gravity, the values of  $\Gamma$  ranging between 0 and 5. The container is made out of 10 mm-thick transparent PMMA walls. The dimensions of the container are denoted  $L_x$ ,  $L_y$  and  $L_z$  respectively along the vibration axis  $x$ , the horizontal transverse axis  $y$  and the vertical axis  $z$ . The vertical walls are labeled north/south, east/west (fig. 1). The granular medium is made of rounded sand grains, composed by more than 99.2% of quartz (controlled by XRD). The number size distribution of the grains, as measured by Laser granulometry, is very well approximated by a skew normal distribution with an average diameter  $\langle d \rangle = 370 \mu\text{m}$ , a standard deviation  $\sigma = 216 \mu\text{m}$

and a skewness of 3.6. The wall-grain friction coefficient has been measured by shear tests performed with a powder rheometer (FT4, Freeman Technology); its value is  $\mu_{wall/grain} = 0.3$ . The heap angle of repose of the granular medium has been experimentally determined and is equal to  $\phi = 30^\circ$ . As it will be established in section 3.4, it corresponds to a numerical grain-grain friction coefficient  $\mu_{grain/grain} = 1$ . Table 1 summarizes these data, as well as other parameters useful for numerical computations like shear ratio  $G = \frac{E}{2(1+\nu)}$  ( $E$ ,  $\nu$ : Young's modulus and Poisson ratio, with standard values for silica sand grains [25]), numerical and viscous damping  $D_n$  and  $D_v$  [26].

The sample preparation protocol consists in pouring the granular medium in the container with the help of a funnel of 2 cm diameter and then flatten the free surface by suction (bed height of  $H_{sand}$ ). Such a protocol generates initial loose packings with a density of  $59.5\% \pm 0.5\%$ .

### 2.2 Experimental data acquisition tools

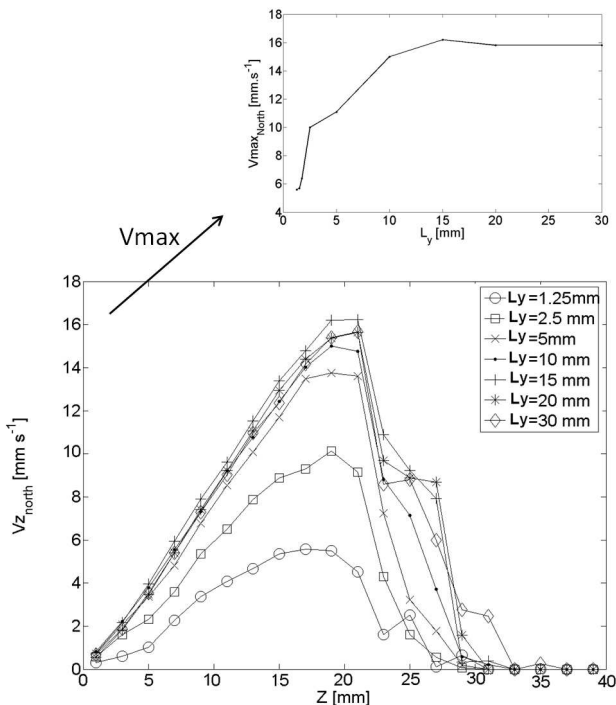
Two main data are used to characterize the state of the vibrated granular medium: the global packing density and the velocity field of the grains moving along the transparent container walls. To accurately measure the global density, we use a confocal optical pen, whose 200  $\mu\text{m}$  diameter light beam scans the free surface of the packing. By integration, we then compute the apparent volume of the granular medium and its global density (averaged density in the granular media). The accuracy of the global density is estimated at 0.5 %, both in dynamic (with vibration) and static conditions. The density measurement device is detailed in [14], where it has been extensively used to analyse the densification of a vibrated sand packing. The 3D grains trajectories can be experimentally measured with sophisticated tools such as Positron Emission Particle Tracking (see Hoomans *et al.* [27]). Here, we have chosen a simpler method, namely the Particle Image Velocimetry. A fast camera takes pictures of the grains at the immediate vicinity of a given face of the recipient at a rate of 50 frames per second, that is to say in phase with the forced oscillations. Then, with a specially designed method, we analyse a set of 50 pairs of images to produce the velocity field. On the north/south walls, this 2D velocity field is "summarized" in a 1D velocity profile, where, for each altitude  $Z$ , we compute the vertical component of the mean grain velocity (the horizontal component is comparatively, negligible).

### 2.3 Modeling method and data analysis approach

The Discrete Element Method is used in this work with the commercial software PFC3D from ITASCA. A sinusoidal horizontal motion is imposed to a rectangular recipient containing a collection of grains. Each grain is modeled by a soft sphere and its position is computed at each time step on the basis of the gravitation force and contact forces that apply on it. For the contact force, we use the standard

**Table 1.** Default main parameters

Parameters			Experimental	Model
Mean grain diameter	$d_g$	[ $\mu\text{m}$ ]	450	900 or 450 (1 exp)
Density	$\rho$	[ $\text{kg m}^{-3}$ ]	2700	2700
Shear ratio	$G$	[MPa]	40	$40 \cdot 10^3$
Poisson's ratio	$\nu$	[-]	0.18-0.27	0.25
Friction coeff.	$\mu_{wall/grain}$	[-]	0.3	0.3
Friction coeff.	$\mu_{grain/grain}$	[-]	?	1 (see sect. 3.4)
Container size	$L_x$	[mm]	40	40
Container size	$L_y$	[mm]	40	periodic
Restitution coeff.	$e$	[-]	0.7	0.7
Viscous damping coeff.	$D_v$	[N.s.m $^{-1}$ ]	-	0.1
Numerical damping coeff.	$D_n$	[-]	0	0.1
Number of grains	$N$	[-]	$max \approx 10^7$	$max \approx 5 \cdot 10^4$

**Fig. 2.** Influence of the size of the periodic cell on the velocity of spheres along the north face and focus on the maximum velocities,  $f=50$  Hz,  $\Gamma = 3$ ,  $L_x=40$  mm

Hertz model with a friction coefficient  $\mu$  and a stiffness coefficient  $k$ . Results of modeling works found in literature are usually difficult to reproduce because the set of parameters is not extensively indicated. Table 1 presents the values chosen in our study. We point out that, numerical simulations have been carried out using a truncated gaussian Particle Size Distribution almost proportional to the real one. The polydispersity offers the advantage of preventing crystallization [28]. When not specified, the mean diameter is twice that of the experimental one to keep the particles number below 80,000 and hence the calculation time under 150 hours. We assume that the difference of

shape does not affect the qualitative behaviour of the system [29]. The initial state is prepared by sedimentation of spheres randomly created in space. After the force balance is reached, the density is measured. It is rather loose with a value of  $59.5\% \pm 0.5\%$ .

In order to represent a wide system with the minimum number of particles (to get a reasonable calculation time), we have used periodic boundary conditions along the horizontal y-axis that is orthogonal to the vibration x-axis. The influence of the size of the periodic side on velocities is shown on fig.2. The minimum length of the unit cell required to avoid finite-size effects appears to be 10 grain diameters. For larger values, the velocity profile along the north face becomes independent of the unit cell size: the container behaves as if the transverse dimension  $L_y$  were infinite, i.e. without the influence of the side walls. Let us remark that the maximal velocity on north face can be considered as one of the most sensitive parameter to the periodic size and we assume that if this scalar remains the same, the global behaviour of the system remains unchanged. The reader can notice that the minimum unit cell size depends on the numerical experiment. For instance, [30] found that a unit cell of 2 grains size is enough for describing the discharge of a rectangular hopper.

Moreover, we have transformed the natively used Lagrangian description (grains are followed individually) into an Eulerian description (continuum described by density-, velocity-, stress-, ... fields) in order to better visualize the modeling results and easily compare them with the experimental ones, especially with the velocity fields. The averaging procedures are standard ones. It should be notice that, in order to smooth the fluctuations due to the chaotic nature of the medium behaviour, the data have been averaged over a series of 10 oscillation periods. The velocity of a grain for one oscillation period has been calculated by considering its displacement during one cycle of vibration and dividing it by the period of the oscillation. Afterwards, the velocities have been averaged in space (eulerian procedure).

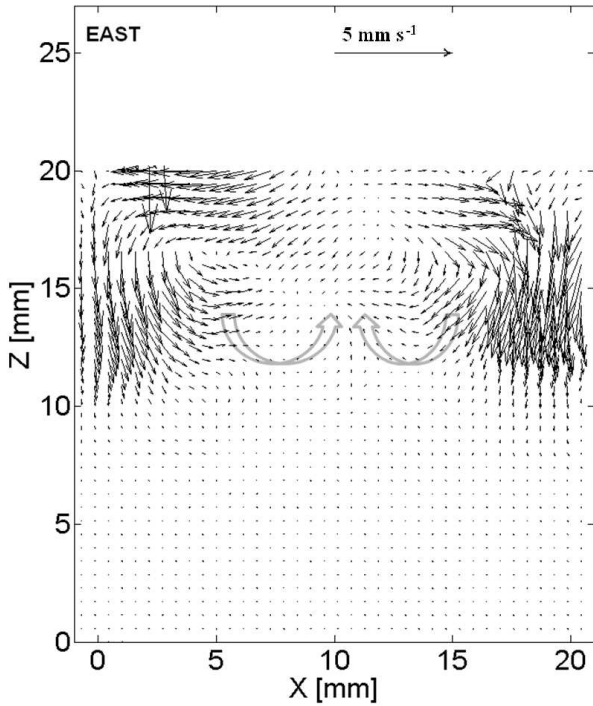


**Fig. 3.** East side view. Velocity field measured experimentally by PIV technique and averaged over 10 cycles of vibrations. Observation of the counter-rotating convection rolls.  $\Gamma = 3$  and  $f = 50$  Hz. In these conditions, the rise of the grains is not located at the wall surface for this acceleration, but in the bulk of the granular packing.  $d_{gexp} = 500 \mu\text{m}$

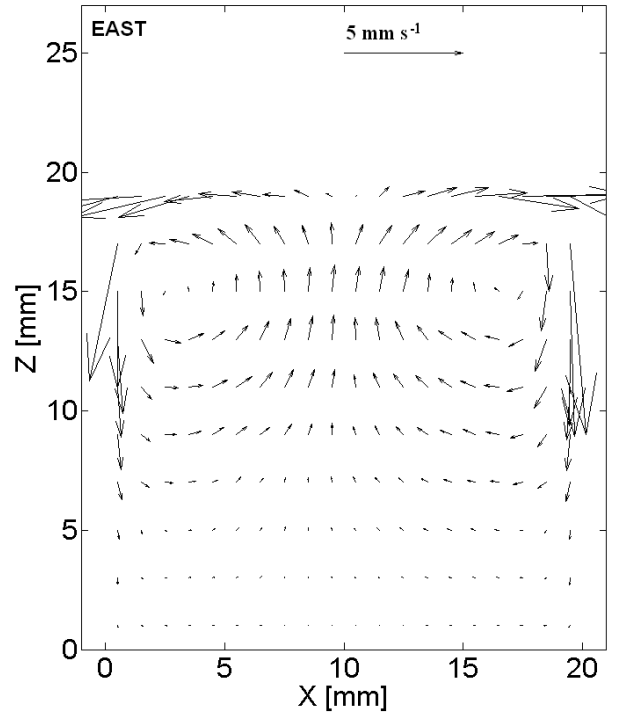


**Fig. 4.** East side view. Numerical velocity field averaged over 10 cycles of vibrations. Observation of the counter rotating convection rolls.  $\Gamma = 3$  and  $f = 50$  Hz.  $d_{gmod} = d_{gexp} = 500 \mu\text{m}$ . Due to periodic boundary conditions, the surface velocity fields coincide with the bulk one.

### 3 Results

We have chosen to study the influence of the dimensionless acceleration  $\Gamma$ , the length  $L_x$  of the vibrated box, and the friction coefficients upon the global packing fraction and the velocities of the grains along the transparent walls of the container. In section 3.1, we present results where the particles diameters in the simulation are the same as in the experiments. In the following sections, the diameter in simulation is twice the experimental one.

#### 3.1 Convective pattern and simulation calibration

For  $f = 50$  Hz and an acceleration above the critical value  $\Gamma = 0.8$  (under which no bulk movement is noticed), the rheological behaviour of the granular medium can be mainly described by two counter-rotating convection rolls in the upper region as described in fig. 1, fig. 3 and fig. 4. This convective motion is driven by the avalanching mechanism: the vibrations imposed along the north-south axis create an intermittent gap between the granular medium and the north or south wall alternatively. Medved *et al.* [31] have studied the existence and evolution of this gap with  $\Gamma$ . By gravity, the grains can fall down into this gap. Then, they penetrate into the bulk, are pushed horizontally by the walls and go upwards in the central part of

the container. When they arrive at the top of the pile, the grains may fall down again and the loop is closed [7].

The validity of the parameters chosen in the model has been checked by two experiments and simulations where most geometrical parameters (size of the grains, width of the box and height of sand, ...) were the same. The only difference is the periodic side created in the simulation. Figure 3 and fig. 4 show respectively the experimental and numerical velocity field averaged over 10 cycles of vibration at  $\Gamma = 3$ ,  $f = 50$  Hz,  $L_x = 20$  mm,  $H_{sand} = 20$  mm, and  $L_y = 40$  mm in experiment and  $L_y = 10$  mm periodic in modeling. The reader will notice that the rise of the grains is evidenced in the simulation (fig. 3) but not in the experiment (fig. 4). Effectively, the grains seem motionless at the surface wall and they go up in the core of the medium. In addition, the extent of the region at rest is larger in DEM than in experiments and is attributed to the difference of grain shape (perfect spheres *vs.* rounded sand grains) and boundary conditions (physical walls *vs.* periodic boundary conditions). Apart from these two differences, with identical diameters, the convective patterns and the order of magnitude of the velocity fields show a good agreement. Figure 5 shows that, for the same diameter, the numerical and experimental velocity profiles along the north face are qualitatively and quantitatively similar (error  $\approx 15\%$  on the maximal velocity on north side). We can point out that for low  $z$ -values, *i.e.* at greater depth, the grain velocity is larger in the numerical simulations

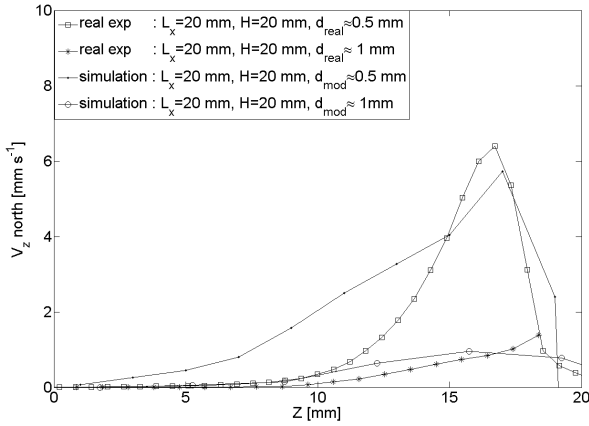


**Fig. 5.** Experimental and numerical velocity profiles for identical sand height and box length at  $\Gamma=3$ ,  $f=50$  Hz

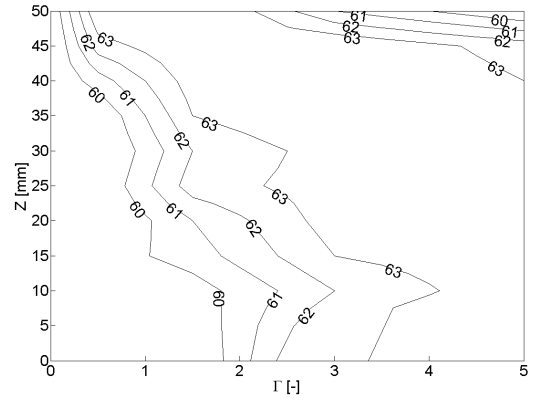


**Fig. 7.** Computed relaxed density [%] as a function of  $Z$  and  $\Gamma$  for  $f=50$  Hz

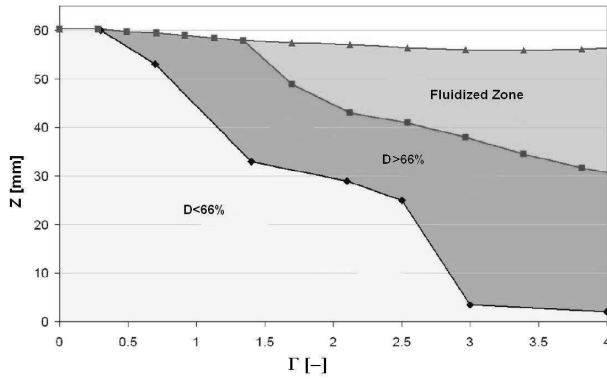


**Fig. 6.** Experimental relaxed density as a function of  $Z$  and  $\Gamma$  for  $f=50$  Hz (from Raihane *et al.*[7])

than in the experiments. We attribute this mobility increase to the spherical shape of the modeled grain that allows them to move more easily by rotation or sliding than it would be with more polyedric grains. It also shows that in the given conditions, multiplying the diameter by two implies a division of the maximal velocity by 7.

In the following sections, to avoid excessively long calculation time, simulations are performed with grains twice as large as the sand grains used in experiments. Therefore, we draw the attention of the reader on the fact that the numerical results exposed in the next sections will give a more qualitative than quantitative description of the granular medium behaviour.

### 3.2 Influence of acceleration on packing properties

#### 3.2.1 Density

##### *Experiments*

On exactly the same system, Raihane *et al.* [14] have measured the local relaxed density of the packing (fig. 6). For low accelerations, it has been shown that the bottom layers remained at the initial density, whereas the upper lay-

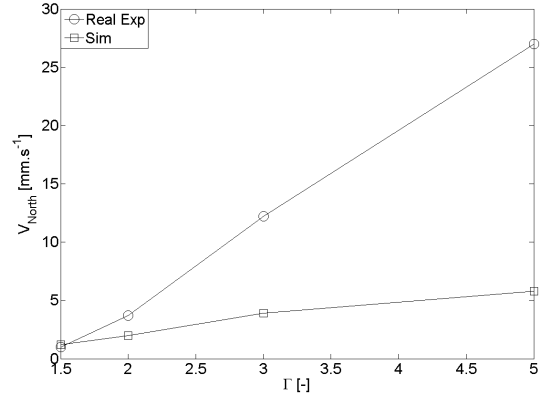


**Fig. 8.** Maximum velocity on north face vs.  $\Gamma$ . Experimental velocities averaged on 50 vibration cycles (standard deviation  $\approx 15\%$ ). Modeled maximum velocity averaged on vibration cycles 90-100 (standard deviation  $\approx 30\%$ ).  $f=50$  Hz,  $L_x=40$  mm,  $H=40$  mm

ers undergo a densification. For higher accelerations, the bottom layers get compacted, but the density decreases in the upper layers. We can explain this latter drop by the fact that the upper grains acquire a significant velocity. In this case, the free volume is enhanced and when vibrations are stopped, the density keeps low.

##### *Simulations*

An assembly of 32000 spheres of density  $C_i = 59.5\%$  is created. This relaxed state can be characterized by the bulk density map (fig. 7). The behavior of the granular packing during the vibrations depends on the acceleration.

For low accelerations ( $\Gamma < 1.5$ ), the density at the bottom of the container remains equal to the initial density. This occurs because the Coulomb criterion has not been reached in this region, which indicates that the compressive stress is high compared to the shear stress.

For high accelerations ( $\Gamma > 3.0$ ), the shear stress is high enough and the Coulomb criterion is fulfilled, even

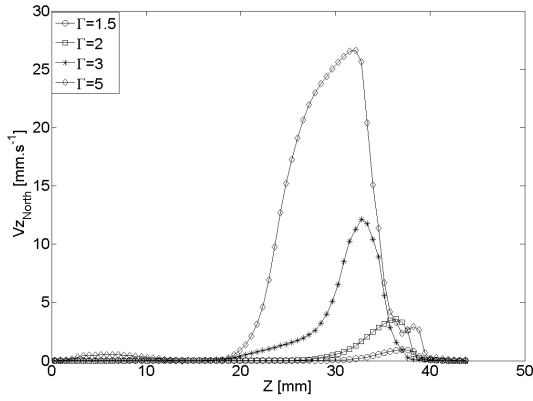


**Fig. 9.** Experimental velocity profile dependence upon  $\Gamma$  for  $f=50$  Hz,  $L_x=40$  mm.

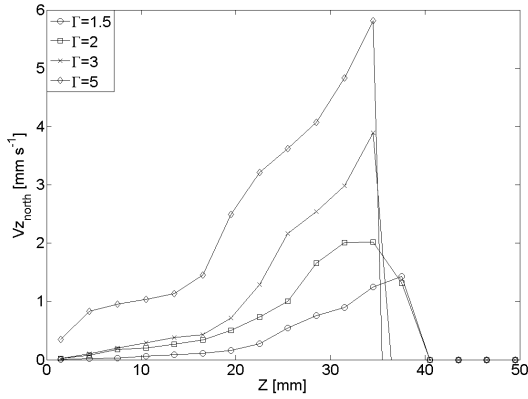


**Fig. 10.** Simulated velocity profile dependence upon  $\Gamma$  for  $f=50$  Hz,  $L_x=40$  mm.

in the deeper layers. Therefore, the grains can move and the packing can densify even at the bottom of the container. In the upper layers, the granular medium becomes fluid and the density decreases.

The local relaxed density increase ranges between 0 % in the jammed bottom layers and 3 % in the fluidized top layers of the packing. The mapping of the density in the dynamic state is given in fig. 7. Experimentally and numerically, we can observe a further small gain in densification ( $max \approx 0.5\%$ ), when vibrations are stopped. Simulation results on the density evolution *vs.* the relative acceleration are in agreement with Raihane [14] experimental data.

### 3.2.2 Velocity of particles at north and south walls

Experiments and simulations have been undertaken in order to obtain the evolution of the maximal velocity along the north face with  $\Gamma$  (fig. 8). Both experimentally and numerically, for  $0 < \Gamma < 5$ , the velocity of the grains increases linearly with the acceleration. We notice a good

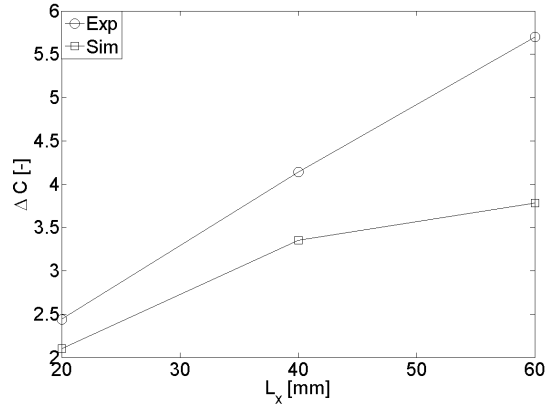


**Fig. 11.** Density increase due to vibrations as a function of  $L_x$ , for  $H_{sand}=60$  mm : experimental and numerical results. Typical error  $\pm 0.5\%$ ,  $\Gamma = 3$ ,  $f=50$  Hz

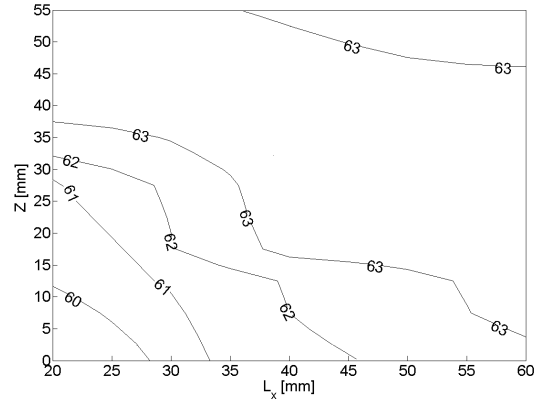


**Fig. 12.** Modeling result : density field as a function of  $L_x$  and  $Z$ ,  $\Gamma=3$ ,  $f=50$  Hz

qualitative agreement between modeling and experimental results (fig. 9 and fig. 10). The quantitative differences between the experimental and computed velocities can be attributed mainly to the size of the grain (double in the model), and secondly to the shape of the grain and the choice of a periodic side  $L_y$  in simulations.

## 3.3 Influence of the container size on the packing properties

### 3.3.1 Density

The granular medium behaviour obviously depends on many parameters. Hereafter, we focus on the influence of the size of the container. Indeed, we have to be cautious when considering the influence of  $\Gamma$  on the bulk dynamic density of the system (fig. 6, fig. 7): these results are valid only for a given container dimension. Numerical simulations and experiments have been performed to evaluate the influence of the length  $L_x$  (measured along the vibration axis) upon the density (fig. 11, fig. 12).



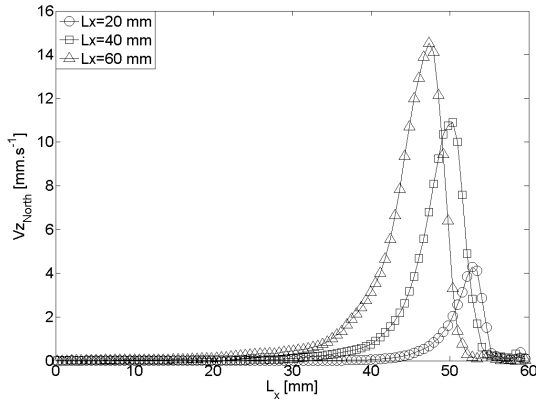


**Fig. 13.** Experimental velocity profile dependence upon  $L_x$  for  $H_{sand} = 60$  mm,  $\Gamma = 3$ ,  $f=50$  Hz

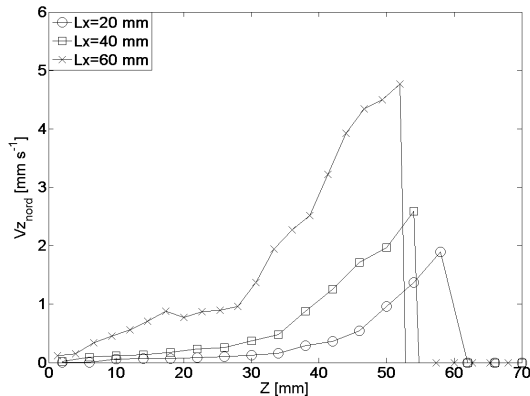


**Fig. 14.** Numerical velocity profile dependence upon  $L_x$  for  $H_{sand} = 60$  mm,  $\Gamma = 3$ ,  $f=50$  Hz

Numerical simulations (fig. 12) show that, for small values of  $L_x$  (20 mm), only the upper layers are compacted, whereas for greater values (starting from  $L_x=60$  mm) all the packing is compacted. This behaviour can be explained by a larger constraint on the displacement of the grains in small containers. Comparing fig.7 and fig.12, we can see that increasing  $L_x$  has got a similar effect to imposing a larger acceleration  $\Gamma$ : the mobility of grains increases and it enables to compact the bottom layers. Experimentally, for  $H_{sand}=60$  mm, we verify that the dynamic or relaxed density increases with the size of the container (fig. 11). The modeling results suggest that the compaction of the bottom layers occurs only if  $L_x$  is long enough. This behaviour explains the experimental evolution of the global density with  $L_x$ .

### 3.3.2 Velocity of particles at north and south walls

For a given bed height ( $H_{sand}=60$  mm), experiments show (fig. 13) that the velocity along the north face and the fluidized zone thickness increases with the size of the con-

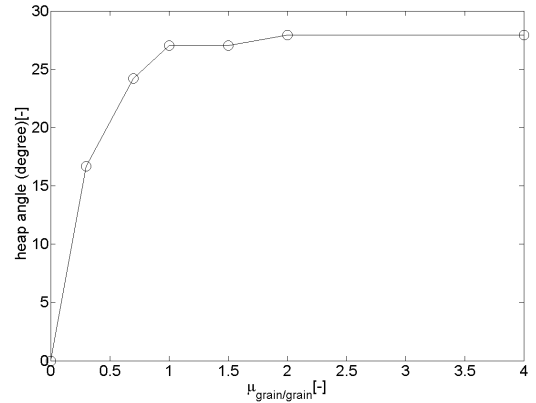


**Fig. 15.** Modeling result : heap angle as a function of the grain/grain friction coefficient imposed in the DEM.

tainer in the range  $L_x=20-60$  mm (Flemmer *et al.* have anticipated this type of behaviour in [32]). For small containers ( $L_x=20$  mm), no motion is observed at the bottom of the container.

In fig. 14, we have plotted the velocity profiles along the north face obtained in simulation. The grain assembly exhibits qualitatively the same behaviour in experimental and modeled systems: the velocity increases with  $L_x$  until  $L_x=60$  mm.

Experimentally and numerically, the velocities can proportionally increase with  $L_x$  (for small values of  $L_x$ ). To explain this phenomenon, we suggest that the steric constraint is weaker when the size of the box increases and the grains can move faster and in the deeper layers. Furthermore, we can state that the geometry and especially the length of the box have an similar influence to that of the acceleration  $\Gamma$  (fig. 9 and fig. 10).

## 3.4 Influence of the friction coefficients on the packing properties

In this section we use simulations to analyze the influence of the friction coefficients  $\mu_{grain/grain}$  and  $\mu_{wall/grain}$  on the packing behaviour.

### 3.4.1 Heap angle

For a given powder, the heap angle depends on many parameters such as the attractive or repulsive forces acting at distance, the friction contact forces due to surface roughness of each individual grains and the contact morphology and associated entanglement. When a specific “real” powder is modeled by perfectly spherical particles, the coefficient of friction  $\mu_{grain/grain}$  must be chosen carefully. One robust way to do so is to adjust this parameter so that the heap angle of the model packing is the same as the experimental one. Experimentally, the heap angle of

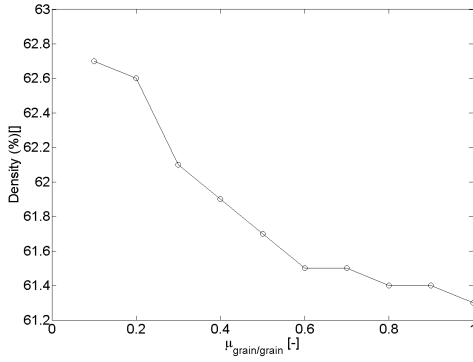


**Fig. 16.** Computed evolution of the dynamic global density *vs.* grain-grain friction  $\mu_{\text{grain/grain}}$

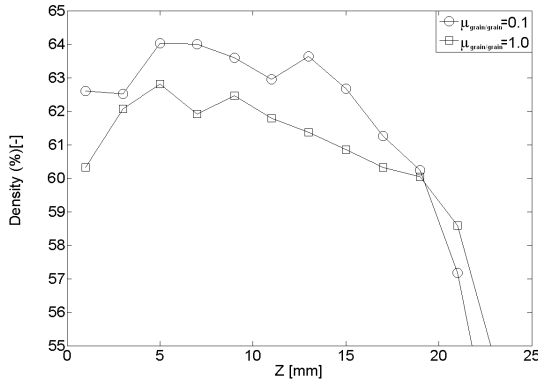


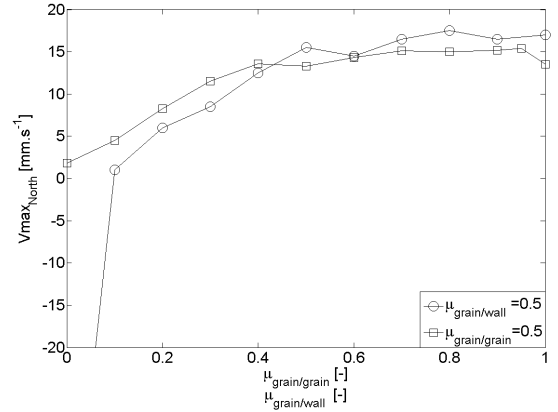
**Fig. 17.** Computed evolution of the dynamic global density profiles for two values of  $\mu_{\text{grain/grain}}$

our sand grains packing has been found to be  $30^\circ$ . We have undertaken a numerical analysis where this angle has been evaluated as a function of the microscopic friction coefficient  $\mu_{\text{grain/grain}}$ . The results plotted on fig. 15 shows that the heap angle increases with  $\mu_{\text{grain/grain}}$  and reaches a plateau for  $\mu_{\text{grain/grain}} \geq 1$ . Hence, we can consider that a coefficient  $\mu_{\text{grain/grain}}$  of 1 gives a good agreement. We did not consider larger values of  $\mu_{\text{grain/grain}}$  because of its poor physical meaning.

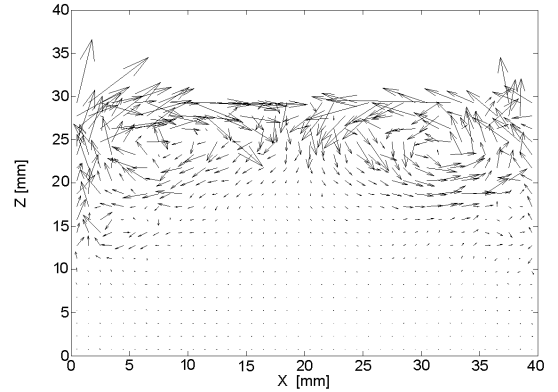
### 3.4.2 Density

Figure 16 shows that the global dynamic density gently decreases with the grain-grain friction coefficient  $\mu_{\text{grain/grain}}$ . We can also see that the density profile is similar for  $\mu_{\text{grain/grain}} = 0.1$  and  $\mu_{\text{grain/grain}} = 1$ .

Let us just notice a global increase of density of approximately 1 % for lower frictional grains (fig. 17). This observations correlates well with Vandewalle *et al.* [33], who experimentally found a difference of 1 % on the relaxed density after compaction between smooth and rough particles. The normalized volume fraction is defined as  $D' = (D - D_0)/(D_{\text{max}} - D_0)$  where  $D$  is the density,  $D_0$  the minimal density, and  $D_{\text{max}}$  the maximal density. Van-



**Fig. 18.** Numerical study of the dependence of the velocities on  $\mu_{\text{grain/grain}}$  and  $\mu_{\text{wall/grain}}$ . When the influence of one friction coefficient is studied, the value of the second coefficient is fixed equal to 0.5.



**Fig. 19.** Calculated velocity field indicating a reverse convection roll for  $\mu_{\text{grain/grain}} = 0$  and  $\mu_{\text{wall/grain}} = 0$ ,  $\Gamma=3$ ,  $f=50$  Hz

dewalle *et al.* also found that  $D'$  does not depend on the friction coefficient of grains (simulation result).

### 3.4.3 Velocity of particle at north and south walls

We have observed that numerical velocities strongly depend on the values of  $\mu_{\text{grain/grain}}$  and  $\mu_{\text{wall/grain}}$ . In fig. 18, one can see that velocities increase sharply with both friction coefficients. An unexpected result is obtained when grain-grain friction coefficient is very low: the velocity becomes negative for  $\mu_{\text{grain/grain}} < 0.1$  (fig. 18) and the convection rolls are reversed (fig. 19). In this case, the grains climb along the north and south walls and fall in the middle of the granular medium. Liffman *et al.* [11] have also shown this type of behaviour, which can be explained by the lack of grain/grain friction coefficient in their model. We can remind that this result is essentially numerical and cannot be reproduced experimentally: at our knowledge, there is no real granular medium with null friction coefficient.

## 4 Conclusion and prospect

In this work, we have shown the strong influence of  $\Gamma$ , the length  $L_x$  of the container, and the friction coefficients on the density and on the velocity fields of a granular medium submitted to horizontal sinusoidal vibrations.

The velocity always increases, when any of these parameters is increased. For high values of  $\Gamma$  and  $L_x$ , a densification of the deepest layers occurs, whereas the surface is fluidized. For low value of  $\Gamma$  and  $L_x$ , densification of surface layers may occur, whereas the bottom layers remain unjammed. The correlation between experimental and modeling results is qualitatively good, but we have to carefully interpret the numerical results. Particularly, it has been shown that the particle size has a large impact on the behaviour of the system. We have also underlined that the friction coefficient may have a major influence on the rheology of the granular medium. Increasing numerically the friction coefficient leads to convection rolls flowing in opposite direction. It is probably not possible to establish such experimental results. However, modeling results suggest that the roughness influences the velocities of the grains. As the influence of the three parameters appears to be qualitatively the same in simulations and experiments, an experimental study of the influence of the roughness on the velocity of the grains would be interesting to verify if the velocities of particles implied in the rolls are affected by friction coefficient. The influence of the grain size has also been suggested by the simulation: a specific study on this size effect would also complete our knowledge. Further studies on the influence of the particle shape are also planned.

## References

1. E.R. Nowak, J.B. Knight, M.L. Povinelli, H.M. Jaeger, and S.R. Nagel. Reversibility and irreversibility in the packing of vibrated granular material. *POWDER TECHNOLOGY*, 94:79–83, 1997.
2. J.B. Knight, C.G. Fandrich, C.N. Lau, H.M. Jaeger, and S.R. Nagel. Density relaxation in a vibrated granular material. *PHYSICAL REVIEW E*, 51(5):3957–3963, May 1995.
3. P. Philippe and D. Bideau. Numerical model for granular compaction under vertical tapping. *PHYSICAL REVIEW E*, 63:051304, 2001.
4. P. Philippe and D. Bideau. Granular medium under vertical tapping: Change of compaction and convection dynamics around the liftoff threshold. *PHYSICAL REVIEW LETTERS*, 91(10):104302, September 2003.
5. A. Raihane, O. Bonnefoy, J.L. Gelet, J.M. Chaix, and G. Thomas. Densification of a 3D granular bed by horizontal vibrations. *XV INTERNATIONAL CONGRESS ON RHEOLOGY - THE SOCIETY OF RHEOLOGY 80th Annual Meeting, AIP Conf. Proc.*, 1027:932–934, 2008.
6. A. Raihane, O. Bonnefoy, J. L. Gelet, J. M. Chaix, and G. Thomas. Experimental study of a 3D dry granular medium submitted to horizontal shaking. *POWDER TECHNOLOGY*, 190(1-2):252–257, 2009.
7. A. Raihane. *Etude du comportement des milieux granulaires vibres horizontalement - Application au remplissage des fusibles*. PhD thesis, Ecole des Mines de Saint-Etienne, 2009.
8. Z. Farkas, P. Tegzes, A. Vukics, and T. Vicsek. Transitions in the horizontal transport of vertically vibrated granular layers. *PHYSICAL REVIEW E*, 60(6):7022–7031, December 1999.
9. D. van der Meer, P. Reimann, K. van der Weele, and D. Lohse. Spontaneous ratchet effect in a granular gas. *PHYSICAL REVIEW LETTERS*, 92(18):184301, 2004.
10. S. G. K. Tennakoon, L. Kondic, and R. P. Behringer. Onset of flow in a horizontally vibrated granular bed: Convection by horizontal shearing. *EUROPHYSICS LETTERS*, 45(4):470–475, 1999.
11. K. Liffman, G. Metcalfe, and P. Cleary. Granular convection and transport due to horizontal shaking. *PHYSICAL REVIEW LETTERS*, 79(23):4574–4576, 1997.
12. M. Medved, D. Dawson, H.M. Jaeger, and S.R. Nagel. Convection in horizontally vibrated granular material. *CHAOS*, 9(3):691–696, September 1999.
13. E. Roueche. *Influence des parametres de vibrations sur la rheologie d'un milieu granulaire : Application au remplissage des fusibles*. PhD thesis, Ecole des Mines de Saint-Etienne, November 2005.
14. A. Raihane, O. Bonnefoy, J. M. Chaix, J. L. Gelet, and G. Thomas. Analysis of the densification of a vibrated sand packing. *POWDER TECHNOLOGY*, 208:289–295, 2011.
15. P. Richard, M. Nicodemi, R. Delannay, P. Ribiere, and D Bideau. Slow relaxation and compaction of granular systems. *NATURE MATERIALS*, 4(2):121–128, February 2005.
16. P.A. Cundall and O.D.L. Strack. Discrete numerical-model for granular assemblies. *GEOTECHNIQUE*, 29(1):47–65, 1979.
17. G. W. Delaney, P. W. Cleary, M. Hilden, and R. D. Morison. Validation of DEM predictions of granular flow and separation efficiency for a horizontal laboratory scale wire mesh screen. In CSIRO, editor, *SEVENTH INTERNATIONAL CONFERENCE ON CFD IN THE MINERALS AND PROCESS INDUSTRIES*, Melbourne, 2009.
18. P.W. Cleary. Large scale industrial DEM modelling. *ENGINEERING COMPUTATIONS*, 21(2-4):169–204, 2004.
19. P.X. Yao, S.C. Yang, L.H. Zhao, and H.L. Lu. DEM simulation of densification in concrete block vibration forming. *2008 10TH INTERNATIONAL CONFERENCE ON CONTROL AUTOMATION ANDROBOTICS, IEEE*, pages 2165–2169, 2008.
20. A.J. Matchett, T. Yanagida, Y. Okudaira, and S. Kobayashi. Vibrating powder beds: a comparison of experimental and distinct element method simulated data. *POWDER TECHNOLOGY*, 107(1-2):13–30, January 2000.
21. J.A.C. Gallas, H.J. Herrmann, and S. Sokolowski. Convection cells in vibrating granular media. *PHYSICAL REVIEW LETTERS*, 69(9):1371–1374, August 1992.
22. J.A.C. Gallas, H.J. Herrmann, and S. Sokolowski. Granular media on a vibrating plate - a molecular dynamics simulation. *INTERNATIONAL JOURNAL OF MODERN PHYSICS B*, 7(9-10):1779–1788, April 1993.
23. J.A.C. Gallas, H.J. Herrmann, T. Poschel, and S. Sokolowski. Molecular dynamics simulation of size segregation in three dimensions. *JOURNAL OF STATISTICAL PHYSICS*, 82(1-2):443–450, January 1996.

24. C. Saluena and T. Poeschel. Convection in horizontally shaken granular material. *EUROPEAN PHYSICAL JOURNAL E*, 1(1):55–59, 2000.
25. A. Sawicki and W. Swidzinski. Elastic moduli of non-cohesive particulate materials. *POWDER TECHNOLOGY*, 96(1):24–32, April 1998.
26. A. Ollagnier, P. Doremus, and D. Imbault. Contact particles calibration in order to use discrete element code. In *EURO PM 2007 PROCEEDINGS, EPMA*, pages 335–360, Toulouse, 2007.
27. B.P.B. Hoomans, J.A.M. Kuipers, M.A.M. Salleh, M. Stein, and J.P.K. Seville. Experimental validation of granular dynamics simulations of gas-fluidised beds with homogenous in-flow conditions using positron emission particle tracking. *POWDER TECHNOLOGY*, 116(2-3):166–177, May 2001.
28. O. Pouliquen, M. Nicolas, and P.D. Weidman. Crystallization of non-Brownian spheres under horizontal shaking. *PHYSICAL REVIEW LETTERS*, 79(19):3640–3643, November 1997.
29. P. Ribiere, P. Richard, D. Bideau, and R. Delannay. Experimental compaction of anisotropic granular media. *THE EUROPEAN PHYSICAL JOURNAL E: SOFT MATTER AND BIOLOGICAL PHYSICS*, 16(4):415–420, 2005.
30. A. Anand, J. S Curtis, C. R Wassgren, B. C Hancock, and W. R Ketterhagen. Predicting discharge dynamics from a rectangular hopper using the discrete element method (DEM). *CHEMICAL ENGINEERING SCIENCE*, 63(24):5821–5830, 2008.
31. M. Medved. Connections between response modes in a horizontally driven granular material. *PHYSICAL REVIEW E*, 65(2), February 2002.
32. R. C. Flemmer and I. J. Yule. Coherence of a packed bed under lateral oscillation. *POWDER TECHNOLOGY*, 171(3):154–156, 2007.
33. N. Vandewalle, G. Lumay, O. Gerasimov, and F. Ludewig. The influence of grain shape, friction and cohesion on granular compaction dynamics. *THE EUROPEAN PHYSICAL JOURNAL E: SOFT MATTER AND BIOLOGICAL PHYSICS*, 22(3):241–248, 2007.